ARMY RESEARCH LABORATORY

$CaLi_2$ as an Anode in Li-Ion Batteries

by Jeff Wolfenstine

ARL-TN-201 April 2003

NOTICES

Disclaimers

The findings in this report are not to be construed as an official Department of the Army position, unless so designated by other authorized documents.

Citation of manufacturers' or trade names does not constitute an official endorsement or approval of the use thereof.

Army Research Laboratory
Adelphi, MD 20783-1197

ARL-TN-201 **April 2003**

$CaLi_2$ as an Anode in Li-Ion Batteries

Jeff Wolfenstine
Sensors and Electron Devices Directorate, ARL

REPORT DOCUMENTATION PAGE

Form Approved
OMB No. 0704-0188

1. REPORT DATE *(DD-MM-YYYY)*	2. REPORT TYPE	3. DATES COVERED (From - To)
April 2003	Summary	August 2002–January 2003

4. TITLE AND SUBTITLE
$CaLi_2$ as an Anode in Li-Ion Batteries

5a. CONTRACT NUMBER

5b. GRANT NUMBER

5c. PROGRAM ELEMENT NUMBER
61102A

6. AUTHOR(S)
Jeff Wolfenstine

5d. PROJECT NUMBER

5e. TASK NUMBER

5f. WORK UNIT NUMBER

7. PERFORMING ORGANIZATION NAME(S) AND ADDRESS(ES)
U.S. Army Research Laboratory
Attn: AMSRL-SE-DC
2800 Powder Mill Road
Adelphi, MD 20783-1197

8. PERFORMING ORGANIZATION REPORT NUMBER
ARL-TN-201

9. SPONSORING/MONITORING AGENCY NAME(S) AND ADDRESS(ES)
U.S. Army Research Laboratory
2800 Powder Mill Road
Adelphi, MD 20783-1197

10. SPONSOR/MONITOR'S ACRONYM(S)

11. SPONSOR/MONITOR'S REPORT NUMBER(S)

12. DISTRIBUTION/AVAILABILITY STATEMENT
Approved for public release; distribution unlimited

13. SUPPLEMENTARY NOTES

14. ABSTRACT
This technical note summarizes the work on $CaLi_2$ as a potential anode for use in Li-ion batteries. $CaLi_2$ was studied for two reasons: (1) $CaLi_2$ has a theoretical gravimetric capacity of 3.6 times the theoretical value of the currently used graphite, and (2) The melting temperature of $CaLi_2$ is 503 K. The ratio of the testing temperature (room temperature), T, to the melting temperature, T_m, for $CaLi_2$ is equal to 0.59. This is significant because it is known that as the ratio of $T/T_m > 0.4$, diffusion processes become important allowing time-dependent plastic deformation to occur, which can accommodate the stresses generated as a result of Li insertion. In contrast, most Li alloys are tested in the region $T/T_m < 0.4$, where no plastic deformation occurs and hence, rapid failure with high capacity fade is observed. It was expected that $CaLi_2$ should exhibit low capacity fade compared to most other Li alloys.

A $CaLi_2$ alloy with micron-sized particles exhibited a rapid loss of capacity with increasing number of cycles. Its rapid failure and capacity fade can be correlated with its low-fracture toughness ($K_{IC} \sim 1$ MPa-$m^{1/2}$). It is anticipated if the particle/grain size can be reduced from the micron to the nanoscale that the material will switch from a dislocation to a grain-sliding deformation mechanism, which will lead to increased ductility and reduced capacity fade. A high ratio of the testing temperature to the melting temperature ($T/T_m > 0.4$) is a necessary but not sufficient condition for an alloy to exhibit low capacity fade. The microstructure must also be considered.

15. SUBJECT TERMS
Li-ion, batteries, anode, calcium, brittle, capacity fade

16. SECURITY CLASSIFICATION OF:			17. LIMITATION OF ABSTRACT	18. NUMBER OF PAGES	19a. NAME OF RESPONSIBLE PERSON
a. REPORT	b. ABSTRACT	c. THIS PAGE			Jeff Wolfenstine
UNCLASSIFIED	UNCLASSIFIED	UNCLASSIFIED	UL	12	19b. TELEPHONE NUMBER *(Include area code)* (301) 394-0317

Contents

List of Figures

Introduction

Recently, there has been renewed interest in the use of metals that alloy with Li as replacement anodes for graphite in Li-ion batteries [1–8]. The major advantage of alloys over graphite is a higher specific reversible capacity that leads to higher energy density batteries. The major problem associated with alloys is the loss of capacity with cycling (capacity fade). Capacity fade results from tensile stresses that occur as a result of the large-volume change upon Li addition. In most alloys, the material cannot accommodate these stresses and hence, fracture rapidly occurs, causing the anode particles to lose contact with the current collector and electrolyte leading to capacity fade. One potential solution to solve the capacity fade problem is to use a composite anode [1–5]. The composite anode consists of an Li-active metal (which upon Li addition forms an alloy) dispersed within an inactive (material that does not alloy with Li) matrix. The purpose of the inactive matrix is to reduce the stresses associated with Li insertion during charging. The disadvantage of the composite anode is the extra weight of the inactive matrix, which reduces the specific capacity of the anode, and hence the energy density of the battery compared to one containing only an Li-active metal anode. Another potential solution is to use a Li active metal that upon alloying with Li, forms a low melting temperature material. In this case, the stresses developed during Li insertion can be accommodated by both instantaneous and time-dependent plastic deformation, thus reducing the tendency to fracture and hence, leading to low-capacity fade. The melting temperature of the alloy should be above the melting temperature of pure Li for safety considerations.

One such Li alloy that meets this criteria that has not received any attention is $CaLi_2$. $CaLi_2$ is the only compound in the Ca-Li system. $CaLi_2$ has a theoretical gravimetric capacity of 1337 mAh/g. This is ~3.6 times the theoretical value of the currently used graphite (372 mAh/g) [9]. Thus, the use of $CaLi_2$ as a replacement for graphite will lead to a higher energy density Li-ion battery. The melting temperature of $CaLi_2$ is 503K (230 °C) [10]. The ratio of testing temperature, T, to the melting temperature, T_m, for $CaLi_2$ corresponds to 0.59, assuming room temperature is the testing temperature. For many Li forming alloys such as $Li_{4.4}Sn$, T/T_m is around 0.30 [10]. This is significant because it is known that as the ratio $T/T_m \geq 0.4$-0.5 diffusion processes become important allowing time-dependent plastic deformation to occur, which can accommodate the stress generated as a result of Li insertion [11–16]. For $T/T_m \leq 0.4$ diffusion processes are not significant enough to allow time-dependent plastic deformation processes to occur and hence, rapid failure results [11–16]. Since $T/T_m = 0.59$ for $CaLi_2$ it is anticipated that plastic deformation will occur at room temperature to help relieve the stress developed during Li insertion, and hence low-capacity fade should be exhibited. In contrast, in most active Li alloys (i.e., $Li_{4.4}Sn$, $Li_{4.4}Si$) plastic deformation will not occur at room temperature and hence, rapid fracture and low rapid capacity fade is expected and observed [1, 3, 8, 9, 17, 26–28]. In addition, the melting temperature of $CaLi_2$ is above that for pure Li (453 K), thus making $CaLi_2$ more attractive than pure Li from a safety viewpoint.

It is the purpose of this technical note to investigate $CaLi_2$ as a potential anode for use in Li-ion batteries.

Experimental

The $CaLi_2$ alloy was prepared by mixing the appropriate amounts of Li (foil; Foote Co.) and Ca (granules; Aldrich Co.) in an Mo crucible. Li foil was wrapped around the Ca granules. The Li-Ca mixture was heated at 400 °C for 2 hr in a glove box having an oxygen concentration and moisture level of < 1 ppm to form a molten alloy. The molten alloy was poured onto a stainless steel cooling plate. This material was crushed, ground, and sieved to < 44 μm. The resulting powders were characterized by x-ray diffraction.

The capacity and cycle life of the $CaLi_2$ powders were evaluated in half-cells at room temperature. $CaLi_2$ positive electrodes were prepared by pressing the powders onto an Ni grid in the glove box. Metallic lithium was used as the negative electrode. Cells were constructed by placing the $CaLi_2$ electrode, Celegard 2300 separator, and lithium foil pressed onto an Ni grid between two 1/8-in-thick polypropylene blocks. The cells were placed in foil-laminate pouches and 4 g of a 1M $LiPF_6$:ethlylene carbonate/dimethyl carbonate/diethyl carbonate (5:4:1 by volume) solution was added. The cells were cycled at a constant current density of 20 $\mu A/cm^2$ between 0.001 to 0.65 V. The upper cut-off voltage corresponds to the open-circuit voltage of the Ca granules vs. pure Li. The Ca granules were pressed into a foil, then polished with a file to remove any surface contamination and rapidly placed into the electrolyte.

Results and Discussion

The x-ray diffraction pattern for the $CaLi_2$ powders is shown in Figure 1. The x-ray diffractions peaks and the corresponding (hkl) planes for $CaLi_2$ are shown. No major Ca or Li peaks were observed in the diffraction pattern. From Figure 1, it can be concluded that the Li-Ca alloy was single-phase $CaLi_2$.

A typical discharge and charge cycle for the $CaLi_2$ powder (no additive was used because the alloy is electronically conductive) at a current density of 20 $\mu A/cm^2$ is shown in Figure 2. From Figure 2, several different regions (significant changes in slope) occur as Li addition (voltage decrease) occurs. The first significant change in slope that occurs is ~0.24 V. According to the phase Ca-Li phase diagram [10], this would correspond to Li addition to pure Ca. The second significant change in slope occurs at ~0.09 V, according to the phase diagram. As further Li addition occurs, the next major change in slope occurs at 0.04, which corresponds to the disappearance of the Ca saturated with Li phase and is associated with single-phase $CaLi_2$. It should be noted that the open-circuit voltage for single-phase $CaLi_2$ was 0.037 V, in close agreement with a voltage of 0.04 determined under dynamic conditions. On Li subtraction (voltage increase), the major changes in slope occur at 0.20, 0.37, and 0.45 V. According to the phase diagram, the region from 0.0 to 0.2 is associated with single-phase $CaLi_2$; at 0.37, the two-phase region of $CaLi_2$ plus Ca saturated with Li; and at 0.45, only single-phase Ca with Li until ~0.65 V where all the Li is extracted.

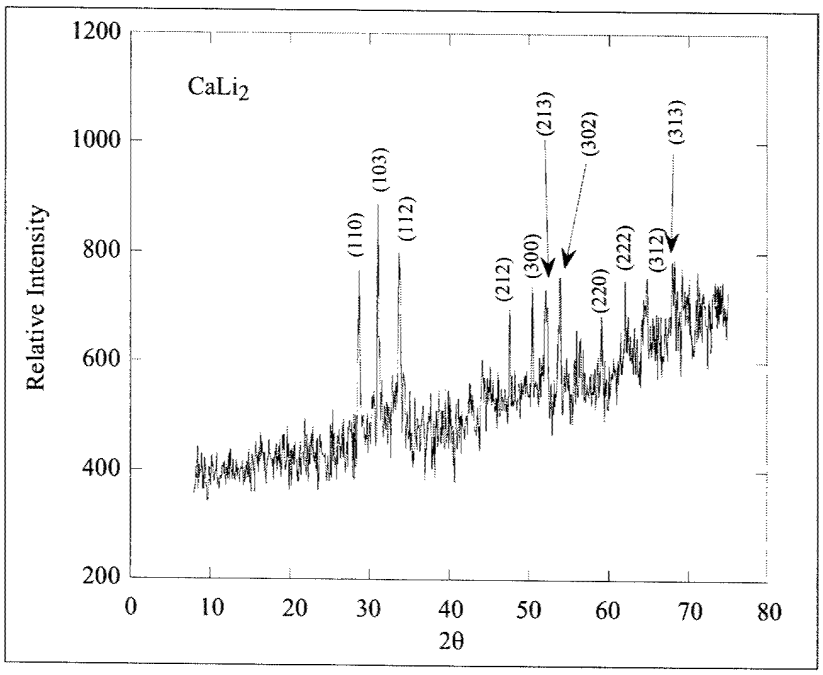

Figure 1. X-ray diffraction pattern of the $CaLi_2$ powders.

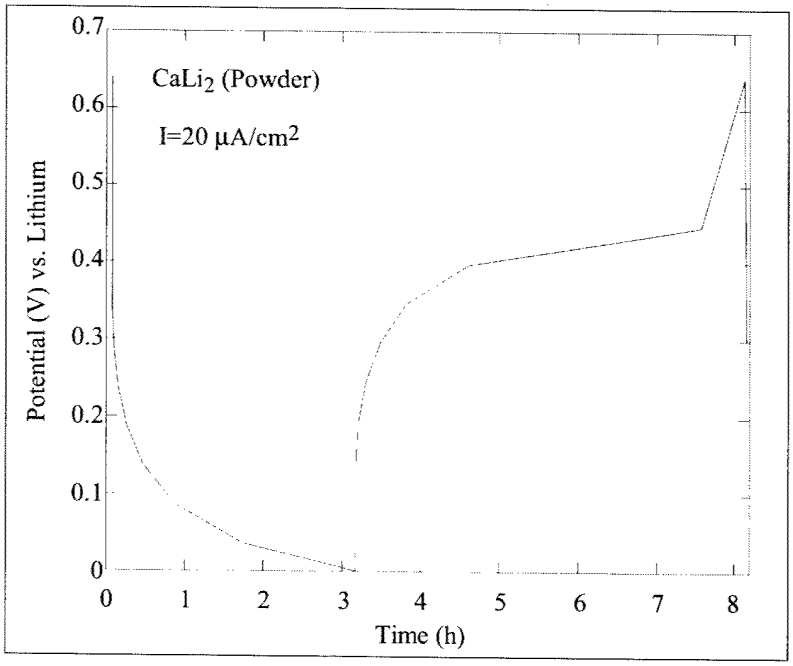

Figure 2. Charge-discharge curve of the $CaLi_2$ powders at room temperature.

The discharge capacity as a function of cycle number for the $CaLi_2$ alloy with no binder or conductive additive is shown in Figure 3. From Figure 3, two important points are noted. First, $CaLi_2$ exhibits a rapid initial capacity fade, which is, followed by a gradual decrease in capacity. For example, it can be seen that the initial capacity on the first cycle is ~300 mAh/g and decays rapidly to 50 mAh/g after 3 cycles, after which it gradually decreases to ~14 mAh/g at the 100th cycle. Second, the experimental observed capacity of $CaLi_2$ is a very low percentage of the theoretical value. For example, at cycle one, it is only 22%, and at the 100th cycle, it is < 1%. The results shown in Figure 3 can be compared to the specific capacity of the presently used graphite anode in Li-ion batteries, which has a practical capacity value of between 300 and 350 mAh/g and exhibits excellent cycle life [17]. It is expected that even if a binder is added to $CaLi_2$ to improve the specific capacity and decrease capacity fade that, even with this addition, the $CaLi_2$ alloy still will not exhibit sufficient specific capacity and reduced capacity fade to become a practical anode for use in Li-ion batteries.

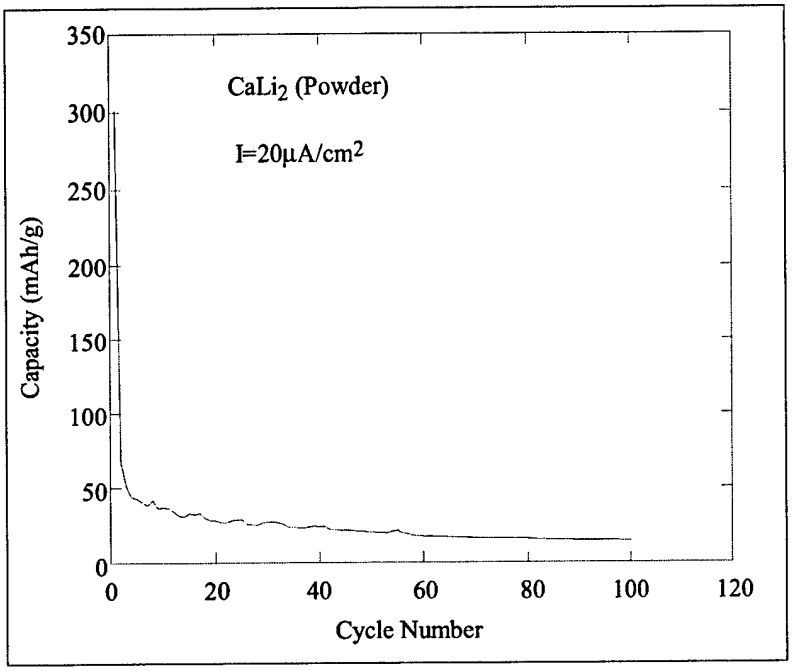

Figure 3. Capacity-vs.-cycle number for $Li/Cali_2$ cell.

A surprising result of this study was the high capacity fade and low-specific capacity of $CaLi_2$ with its high T/T_m. As stated earlier, it was expected because of its $T/T_m > 0.4$ that $CaLi_2$ would show extensive plastic deformation at room temperature to relieve the tensile stress generated as a result of Li insertion and not exhibit rapid fracture and low capacity fade. Instead, $CaLi_2$ exhibited completely brittle behavior with rapid capacity fade with Li insertion. In order to further investigate this phenomenon, the fracture toughness, K_{IC}, of this alloy was experimentally determined, using an indentation technique [18–21]. The K_{IC} for $CaLi_2$ was determined to be ~1 MPa-$m^{1/2}$. K_{IC} values for the ideal brittle material (glass) are close to unity [22–25]. The K_{IC} result, confirm the brittle nature of the $CaLi_2$ alloy. From the K_{IC} results, it has recently been shown by Wolfenstine [26, 27] and latter by Huggins and Nix [28] that for a single-phase alloy

to exhibit low capacity fade that the particle/grain size, X, must be less than a critical particle/grain size, X_c, ($X < X_c$) where X_c is given by the following expression [26, 28]:

$$X_c = 40\ (K_{IC}/E)^2\ (V/\Delta V)^2, \quad (1)$$

where E is the elastic modulus, ΔV is the volume change associated with Li insertion, and V is the initial volume. The volume change divided by the initial volume, $\Delta V/V$, from Ca to $CaLi_2$ is 1.28 per atom of Ca. Inserting this value into equation 1 with E ~ 100 GPa [26] and K_{IC} ~ 1 MPa-$m^{1/2}$ yields X_c ~ 3 nm. The particle size, X, of the $CaLi_2$ powders ~20 μm. In this case, X/X_c ~ 7,000 and hence, rapid fracture and capacity fade is predicted from equation 1 and was observed.

It is of interest to determine why the $CaLi_2$ alloy with $T/T_m > 0.4$ exhibited completely brittle behavior with no evidence for plastic deformation. There are several possible reasons: (1) the crystal structure is hexagonal [10], which restricts the number of slip systems for dislocation motion and hence, limited ductility is expected compared to one with a cubic crystal structure [23], and (2) the complex crystal structure of $CaLi_2$ makes it hard to move dislocations and hinders diffusion, both of which promote limited ductility [11, 12, 14, 16, 23, 25]. One potential solution to overcome the previously mentioned limitations and obtain plastic deformation and low capacity fade at room temperature is to make the $CaLi_2$ alloy nanoscale (particle sizes <100 nm). It is known that as the particle/grain size decreases from the micron to the nanoscale range, this change increases the number of grain boundaries resulting in grain boundary sliding becoming the dominant deformation mechanism in the nanoscale material [12–16]. In this case, the problems of a limited number of slip systems and difficulty in moving dislocations are irrelevant in the nanoscale material deforming by grain boundary sliding. Furthermore, it has been observed that the activation energy for diffusion along a grain boundary is much lower than that for lattice diffusion in many materials [13–15, 29, 30]. Thus, it is possible that $CaLi_2$ tested at room temperature ($T/T_m = 0.59$), whose diffusion is controlled by lattice diffusion in the micrometer range will exhibit a change to diffusion controlled by the grain boundary in the nanoscale range and hence, an enhancement in the diffusion rate will be exhibited as the particle/grain size is reduced and higher ductility and lower capacity fade will be observed.

Conclusions

A $CaLi_2$ alloy with micron-sized particles exhibited a rapid loss of capacity with increasing number of cycles. The rapid capacity fade and brittle behavior can be correlated with its low-fracture toughness (K_{IC} ~ 1 MPa-$m^{1/2}$). It is expected if the particle/grain size can be reduced from the micron to the nanoscale that the material will switch from a dislocation to grain sliding deformation mechanism, which will lead to increased ductility and reduced capacity fade. A high ratio of the testing temperature to the melting temperature ($T/T_m > 0.4$) is a necessary, but not sufficient, condition for anode material to exhibit low capacity fade. The microstructure must also be considered.

References

1. Winter, M.; Besenhard, J. O. *Electrochimi. Acta* **1999**, *45*, 31.
2. Crosnier, O.; Devaux, X.; Brousse, T.; Fragnanaud, F.; Schleich, D. M. *J. Power Sources* **2001**, *188*, 97–98.
3. Yang, J.; Wachtler, M.; Winter, M.; Besenhard, J. *Electrochem. Solid State Lett.* **1999**, *2*, 161.
4. Fang, L.; Chowdari, B. V. R. *J. Power Sources* **2001**, *181*, 97–98.
5. Crosnier, O.; Brousse, T.; Devaux, X.; Fragnanud, P.; Schleich, D. M. *J. Power Sources* **2001**, *169*, 94.
6. Boukamp, B. A.; Lesh, G. C.; Huggins, R.A. *J. Electrochem. Soc.* **1981**, *128*, 725.
7. Wang, G. X.; Sun, L.; Bradhurst, D. H.; Zhong, S.; Dou, S. X.; Liu, H. K. *J. Power Sources* **2000**, *88*, 278.
8. Wang, C.; Appleby, A. J.; Little, F. E. *J. Power Sources* **2001**, *93*, 174.
9. Huggins, R. A. *Solid State Ionics* **2002**, *61*, 152–153.
10. Massalski, T. B. *Binary Alloy Phase Diagrams*; ASM International: Metals Park, OH, 1990; p. 924.
11. Frost, H. J.; Ashby, M. A. *Deformation-Mechanism Maps*; Pergamon Press: New York, 1982.
12. Hertzberg, R. W. *Deformation and Fracture Mechanics of Engineering Materials*; J. Wiley and Sons: New York, 1995.
13. Sherby, O. D.; Burke, P. G. *Prog. Mater. Sci.* **1967**, *13*, 325.
14. Burton, B. *Diffusional Creep of Polycrystalline Materials*; Trans. Tech.: Aedermansdorf, Switzerland, 1977.
15. Mukherjee, A. K.; Bird, J. E.; Dorn, J. E. *Trans. ASM* **1969**, *62*, 155.
16. Cannon, W. R.; Langdon, T. G. *J. Mater. Sci.* **1988**, *23*, 1.
17. Takamura, T. *Solid State Ionics*, **2002**, *19*, 152–153.
18. Anstis, G. R.; Chantikul, P.; Lawn, B. R.; Marshall, D. B. *J. Am. Ceram. Soc.* **1981**, *64*, 533.
19. Chantikul, P.; Anstis, G. R.; Lawn, B. R.; Marshall, D. B. *J. Am. Ceram. Soc.* **1981**, *64*, 539.
20. Niihara, K.; Morena, R.; Hassleman, D. P. H. *J. Mater. Sci. Lett.* **1982**, *1*, 13.
21 Li, Z.; Ghosh, A.; Kobayashi, A. S.; Bradt, R. C. *J. Am. Ceram. Soc.* **1989**, *72*, 904.
22. Barsum, M. W. *Fundamentals of Ceramics*; McGraw-Hill: New York, 1997.

23. Davidge, R. W. *Mechanical Behavior of Ceramics*; Cambridge University Press: Cambridge, UK, 1979.

24. Callister, W. D. *Materials Science and Engineering*; John Wiley and Sons: New York, 1997.

25. Chiang, Y.-M.; Birnie, D.; Kingery, W, D, *Physical Ceramics*; John Wiley and Sons: New York, 1997.

26. Wolfenstine, J.; Foster, D.; Read, J.; Behl, W. K.; Luecke, W. *J. Power Sources* **2000**, *87*, 1.

27. Wolfenstine, J. *J. Power Sources* **1999**, *79*, 111.

28. Huggins, R. A.; Nix, W. D. *Ionics* **2000**, *6*, 57.

29. Evans, R. W.;Wilshire, B. *Introduction to Creep*; The Institute of Materials: London, UK, 1993.

30. Shewmon, P. *Diffusion in Solids*; The Minerals, Metals and Materials Society: Warrendale, PA, 1989.